Heterotopic vascularized murine cardiac transplantation to study graft arteriopathy

Tomomi Hasegawa, Scott H Visovatti, Matthew C Hyman, Takanori Hayasaki & David J Pinsky

Departments of Internal Medicine, Molecular and Integrative Physiology, and the University of Michigan Cardiovascular Center, Ann Arbor, Michigan 48109, USA. Correspondence should be addressed to D.J.P. (dpinsky@umich.edu).

Published online 15 March 2007; doi:10.1038/nprot.2007.48

The development of microsurgical techniques has facilitated the establishment of fully vascularized cardiac transplantation models in small mammals. A particularly useful model that has evolved for the study of cardiac allograft vasculopathy (CAV) is a heterotopic (abdominal) vascularized murine cardiac transplantation model. Using this model has permitted the elucidation of genetic, immune and non-immune factors contributing to the development of this inexorable pathological condition, which compromises half of all human cardiac transplants. This protocol details methods for performing the transplant, histomorphometric assessment of the graft vasculature and functional evaluation of the transplanted heart. In experienced hands, the surgical procedure requires approximately 75 min to complete, and vasculopathy results are obtained at 2 months. This model entails a fully vascularized implantation technique in which the donor ascending aorta and pulmonary artery are sutured end-to-side to the recipient abdominal aorta and inferior vena cava, respectively. As this model reliably reproduces immunological and non-immunological features of CAV, investigators can thoroughly explore contributory mechanisms, diagnostic modalities and therapeutic approaches to its mitigation.

INTRODUCTION

In recent years, cardiac transplantation has become the treatment modality of choice for eligible patients with end-stage heart failure[1]. With the development of more potent and specific immunosuppressives, the 1-year survival rate of transplant recipients has risen to as high as 80–90% (ref. 2). Despite this, improvements in long-term patient survival have been hampered by the inexorable development of cardiac allograft vasculopathy (CAV). CAV is a rapidly progressing form of atherosclerosis that often leads to reduced blood flow and ischemia of distal tissues. As many as 10–12% of transplant recipients develop CAV each year, making CAV the leading cause of death in patients more than 5 years after transplantation[3]. Identifying the development of CAV is difficult, as the denervated heart reliably produces neither the chest pain nor the electrocardiographic changes that typically accompany myocardial ischemia[4]. As a result, vascular disease in the transplanted heart frequently goes unnoticed or is misdiagnosed. The likely sequelae of undiagnosed ischemia in this population include sudden death or cardiomyopathy requiring attempted re-transplantation, which is sometimes not possible because of scarce donor organ availability. For these reasons, enabling models for the study of cardiac allograft transplantation and the pathobiology of CAV are of critical importance.

Histologically, CAV presents as a complex interplay between proliferative myoblasts, macrophages and T lymphocytes leading to the formation of a neointima[5,6]. Though this disease shares features with atherosclerosis, it is distinct in many ways. Among the primary differences is that the lesions of CAV are concentric and diffuse throughout the entire coronary vasculature, though most prominently in the distal vessels. In contrast, atherosclerosis tends to have discrete plaques located near bifurcations in the coronary arteries. The neointima of CAV rarely breaks through the internal elastic lamina (IEL), and calcifications are rarely appreciated on histological examination, which is in direct contrast with atherosclerosis. Another key difference is the time course over which these two vascular diatheses arise: atherosclerosis evolves over a lifetime whereas CAV can develop within a year[5,7,8].

The models

Historical development of animal models: Since the publication of Bernard's landmark report, orthotopic cardiac transplantation has become a well-established and commonly utilized technique for clinical cardiac transplantation in humans[9]. Heterotopic cardiac transplantation was developed in the laboratory for experimental applications and offers several advantages over the orthotopic procedure. As it does not require cardiopulmonary bypass, heterotopic cardiac transplantation is not as technically demanding. In addition, it offers improved accessibility for biopsies, and an increased likelihood of post-procedure survival, even in the setting of graft rejection[10]. In 1905, Carrel and Guthrie pioneered cardiac transplantation in dogs[11]. They transplanted the heart of a puppy into the neck of an adult dog by anastomosing the ligated ends of the carotid artery and jugular vein of the recipient to the donor's aorta, pulmonary artery, one of the vena cavae and a pulmonary vein. The transplanted heart survived for 2 h before failing owing to thrombus formation. In 1933, Mann *et al.* reported a simplified transplantation technique in which the aorta and the pulmonary artery of the donor were anastomosed in an end-to-side fashion to the common carotid artery and the external jugular vein of the recipient[12]. The transplanted hearts survived for 8 d after transplantation, and the donor graft was noted to have provoked an immunological response in the recipient. Subsequently, several investigators transplanted dog and rabbit hearts, with improved survival rates[13–17].

Importance of a vascularized model: Before the introduction of a viable, fully vascularized cardiac transplant model, a technique utilizing the transplantation of a non-vascularized heart was developed by Fulmer *et al.*[18] and refined by Judd *et al.*[19] In this model, neonatal murine cardiac tissue was implanted s.c. into a

pouch formed in the pinna of the ear of a recipient mouse without direct vascular anastomosis. Graft viability of the ear–heart transplantation was evaluated by assessing the presence of autonomous beating, as determined by visual inspection or electrocardiography. The simplicity of the ear–heart transplant technique made it a good method for assessing the immunosuppressive effects of drugs administered to suppress acute allograft rejection[20,21]. However, the non-vascularized model is unsuitable for studies of CAV after cardiac transplantation owing to the lack of coronary flow, and hence the failure to simulate the hydrodynamic blood–endothelial interface of human cardiac allotransplants.

The most important feature of the vascularized model is that in human CAV, there is a general consensus that the endothelium serves as a target for immune attack. This is not surprising as endothelium sits at the nexus of blood and extravascular tissues. It actively regulates nutrient homeostasis (substrate delivery and waste removal), maintains blood fluidity through its effects on thrombosis, fibrinolysis and platelet aggregation and modulates leukocyte traffic. In cardiac transplantation, the development of a diffuse, concentric narrowing of coronary vessels provides evidence that the vascular endothelium is indeed a target of the alloimmune response[22]. Damage to the endothelium can trigger arterial inflammation, thrombosis, vasoconstriction and vascular smooth muscle proliferation, resulting in intimal hyperplasia. The mechanism for the development of CAV is multifactorial and likely includes both immunological triggers (cytokines, inflammatory mediators, complement, leukocyte adhesion molecules) and non-immunological triggers (ischemia-reperfusion injury). All of these factors interact within the transplanted vessels at the blood–endothelial interface, making a vascularized cardiac transplantation model imperative for the study of CAV.

The development of microsurgical techniques facilitated the development of fully vascularized cardiac transplantation in small animals. Abdominal heterotopic cardiac transplantation in rats was first described by Abbott *et al.* in 1964 (ref. 23). This technique established circulation to the transplanted heart by end-to-end anastomoses of the donor aorta and pulmonary artery to the recipient abdominal aorta and inferior vena cava (IVC), respectively. To avoid the complications of paraparesis and paraplegia, Ono and Lindsey modified the technique to incorporate end-to-side anastomoses of the vessels using nylon monofilament sutures[24]. The coronary perfusion circuit in this model was a modified version of Mann's model, in which the transplanted heart was perfused antegradely from the recipient abdominal aorta, which drained into the recipient IVC via the coronary sinus, right atrium, right ventricle and pulmonary artery.

A murine heterotopic cardiac transplantation model was introduced by Corry *et al.* in 1973 (ref. 25), and it continues to be used today. In this model, the donor ascending aorta was anastomosed end-to-side to the recipient abdominal aorta, and the donor pulmonary artery was anastomosed in an end-to-side fashion to the recipient IVC (a procedure similar to the Ono–Lindsey model in the rat). The murine heterotopic cardiac transplantation model requires a higher level of microsurgical technical skill than the rat model. However, the murine model is more useful for the investigation of CAV owing to the availability of a large number of genetically well-characterized transgenic and gene-knockout strains. Furthermore, mAbs and other immunological reagents suitable for use in mice are available in large quantities. The major limitation of the Corry technique in mice is the lack of what is known as 'volume loading' of the left ventricle (LV); the LV, though it contracts, does so with minimal flow impedance or volume ejection, and thus the model may not be truly representative of the physiology found in an orthotopic transplantation[26]. Nevertheless, this model has been accepted as a reliable tool for the assessment of CAV and is in widespread use for this purpose.

Details of the heterotopic cardiac transplant model

Development: Though the basis for work in our laboratory has been the models described above, particularly the Corry model, we have evolved various useful adaptations that are now fully detailed in this protocol. The fully vascularized murine heterotopic cardiac transplantation model allows for either of two different sites of transplantation, abdominal or cervical, or both to be used experimentally. Using a cuff technique, the murine cervical heterotopic cardiac transplantation model was introduced in 1991 (refs. 27,28). Compared with the cervical model, the abdominal model requires a more complex and time-consuming technique[29], though many labs (including our own) prefer the abdominal model for reasons of experience and the ability to reproducibly model CAV with a stable procedure and limited experimental variables. In our early experience, we performed murine heterotopic cardiac transplantation with the anastomotic sites of the donor aorta and pulmonary artery placed in parallel, and with the left side of the pulmonary–IVC suture line accessed from within the lumen. This method presented some technical difficulties because of the pulmonary–IVC anastomosis, which often caused bleeding, stenosis and occlusion at the anastomotic site. Therefore, we recently modified the anastomotic technique according to Niimi's report, which described one of the simplest techniques for a murine model[30]. The hallmark of the modified method is that the anastomotic site of the donor pulmonary artery should be separated from that of the donor aorta and not placed in parallel. This modification has recently enabled us to achieve CAV reliably with fewer technical difficulties[31].

Immune barrier considerations: The immunological basis of tissue rejection was investigated extensively by Medawar *et al.* in 1944 (ref. 32) and many subsequent investigators have found that the intensity of the anti-donor response is proportional to the genetic disparity between donor and recipient. In the cardiac allograft, the MHC is used to predict genetic disparity or similarity. In humans, the MHC molecule is the human leukocyte antigen, whereas in mice it has been designated 'H-2'. Donor MHC antigens can trigger graft rejection by interacting directly with recipient T cells, or indirectly as donor MHC–derived peptides expressed on recipient MHC molecules[33]. For the murine model of heterotopic cardiac transplantation, the mouse strain combination, and thus the differences between the strains at the MHC I and II loci, is the most critical element driving the development of immune-mediated CAV. At present, four types of strain combinations are used[34]: (i) complete histocompatibility; (ii) class I differences only; (iii) class II differences only; and (iv) only minor histocompatibility differences. Among the best-characterized minor histocompatibility differences is the H-Y antigen, which was originally discovered as a sex-linked transplantation antigen by Eichward *et al.*[35] Females of the C57BL/6J (H-2^b) mouse strain rapidly rejected primary syngeneic male grafts; however, not all recipients experienced rejection

in the setting of the H-Y mismatch[36,37]. Thus, we usually select the total allo-mismatch combination of the C57BL/6J (H-2^b) strain and the B10A (H-2^a) strain or the C57BL/6J (H-2^b) strain and the CBA/J (H-2^k) strain in male mice for the investigation of CAV development in murine heterotopic cardiac transplantation.

A general overview of the procedure can be viewed in **Figure 1**.

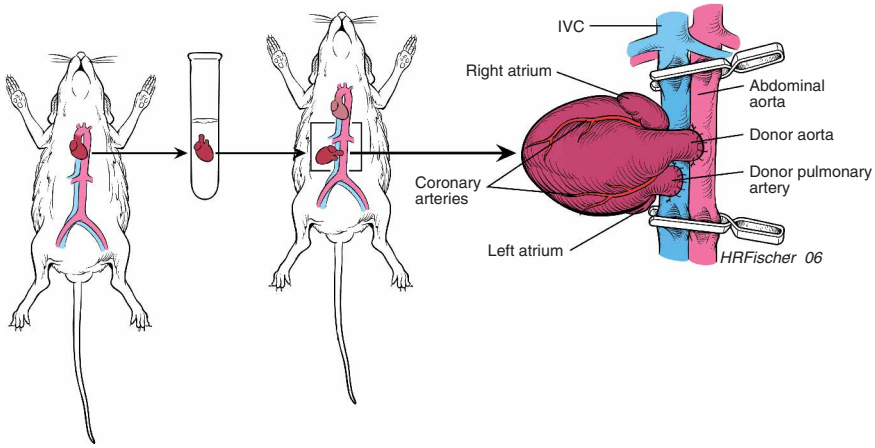

Figure 1 | Overview of heterotopic murine cardiac transplant model.

MATERIALS

REAGENTS

- Male C57BL/6J (H-2^b), B10A (H-2^a) and CBA/J (H-2^k) mice, Jackson Laboratories (Bar Harbor, ME) ! **CAUTION** All experiments involving animals must be performed according to national and institutional regulations. This protocol has been approved by the University of Michigan Committee on Use and Care of Animals for use by the authors. ▲ **CRITICAL** All mice should be between 8 and 12 weeks of age and weigh 25–35 g.
- Ketamine (50 mg kg^{-1})
- Xylazine (10 mg kg^{-1})
- Heparin solution (100 U ml^{-1}) (see REAGENT SETUP)
- Preservation solution (see REAGENT SETUP)
- Saline solution (0.9% sodium chloride; Abbott Labs, cat. no. NDC 0074-7983-61)
- 10% formaldehyde (see REAGENT SETUP)
- 1× PBS is prepared by diluting 10×PBS (GIBCO, cat. no. 14200-075) with dH_2O
- ACCUSTAIN Harris hematoxylin solution, modified (Sigma-Aldrich, cat. no. HHS16-500ML)
- ACCUSTAIN eosin Y solution alcoholic (Sigma-Aldrich, cat. no. HT110116-500ML)
- ACCUSTAIN elastic stain kit (Sigma-Aldrich, cat. no. HT25A-1KT)

EQUIPMENT

- Microscope (WILD M691 or M651, Leica Microsystems, Inc., Allendale, NJ)
- Coagulator (Malis Bipolar Coagulator & Bipolar Cutter CMC II, Codman & Shurtleff, Inc., Randolph, MA)
- Needle holder (HALSEY, Roboz Surgical Instruments, cat. no. RS-7840)
- Large micro-tweezer (Roboz Surgical Instruments, cat. no. RS-5041)
- Large micro-tweezer with 45° angle (Roboz Surgical Instruments, cat. no. RS-4951)
- Small micro-tweezer (Roboz Surgical Instruments, cat. no. RS-4966)
- Small micro-tweezer with 45° angle (Roboz Surgical Instruments, cat. no. RS-5005)
- Micro-spring scissors (VANNAS, Roboz Surgical Instruments, cat. no. RS5618)
- Micro-retractor (MURDOCK, Roboz Surgical Instruments, cat. no. RS-6550)
- Micro-clip (Roboz Surgical Instruments, cat. no. RS-5431)
- Clip-applying forceps (Roboz Surgical Instruments, cat no. RS-5440)
- Micro-bipolar forceps (JEWELERS, ASSI, cat. no. 10-3002-BPI)
- 5-0 silk (Roboz Surgical Instruments, cat. no. SUT-15-1)
- 5-0 nylon on 16-mm (3/8) needle (Sharpoint DR16, Surgical Specialties Co., cat. no. AC-0556N)
- 10-0 nylon on 4-mm (3/8) needle (Sharpoint DR4, Surgical Specialties Co., cat. no. AK-2120)
- Absorbable gelatin sponge (Gelform, Harvard Apparatus, cat. no. 59-9863)
- 1-ml syringe with 27-gauge needle (Becton Dickinson Labware, cat. no. 309623)
- 30-gauge needles (Becton Dickinson Labware, cat. no. 305106)
- Hewlett-Packard SONOS 5500 ultrasound system (Philips, Andover, MA) or Vevo 770 micro-imaging system (Visualsonics, Toronto, Canada) with 12 MHz or greater transducer
- Infusion pump (KD Scientific, cat. no. KDS-100)
- Surflo winged cannula (Terumo Co., cat. no. SV*21BLK)
- Sony DXC-960 MD 3CCD color camera affixed atop an Olympus imaging microscope
- Interactive image analysis system (Image Pro-Plus, version 4.5, MediaCybernetics, Silver Spring, MA) installed on a Pentium IV PC
- The microsurgical equipment listed above represents our preference, but with the correct focal distances, other setups are equally likely to be effective.

REAGENT SETUP

Pre-operative immunosuppression Pre-operative immunosuppressives are administered to recipient mice to achieve reproducible, indefinite graft survival. The immunosuppression is provided by a brief course of treatment with antimurine CD4 (clone GK1.5) Abs and antimurine CD8 (clone 2.43) Abs. Each of them is administered via i.p. injection at 6, 3 and 1 d before transplantation, using 0.2 ml fluid containing 1.5 mg ml^{-1} each mAbs[38,39]. Both anti-CD4 and anti-CD8 Abs are prepared as IgG from hybridoma clones by a commercial vendor (Harlan Bioproducts for Science, Inc., Indianapolis, IN). There is no subsequent immunosuppressive treatment after transplantation.

Heparin solution Prepared by diluting heparin (1,000 U ml^{-1}; Baxter Healthcare, cat. no. NDC 0641-2440-41) in saline solution.

Preservation solution A commercially available buffered electrolyte solution (Electrolyte Solution for Preservation; Baxter Healthcare, cat. no. NDC 0941-0473-21) is typically used, unless it is the preservation solution itself that is to be studied.

10% formaldehyde is prepared by diluting 37% formaldehyde solution (Fisher, cat. no. BP531-500) in 1× PBS.

PROCEDURE

Donor operation ● TIMING 6–7 min

1| Anesthetize the C57BL/6J (H-2^b) mouse with i.p. ketamine (50 mg kg^{-1}) and xylazine (10 mg kg^{-1}).

2| Place the mouse under an operating microscope at ×6–10 magnification.

3| Make a midline abdominal incision.

4| Inject 0.5 ml heparin solution (100 U ml^{-1}) into the IVC using a 1-ml syringe with 27-gauge needle.

5| After 1 min for the systemic heparinization, extend the incision cephalad through a median sternotomy.

6| Separate the anterior chest wall from the diaphragm and retract bilaterally using two-curved mosquito forceps.

7| Free the heart from the surrounding tissue and resect the thymus.

8| Ligate the IVC and the right superior vena cava (SVC) using a 5-0 silk suture near the atrium.

9| Using micro-spring scissors, transect the ascending aorta below the brachiocephalic artery.

10| Transect the main pulmonary artery as distally as possible.

11| Ligate the pulmonary veins and the left SVC *en bloc* using 5-0 silk proximally.

12| Harvest the donor heart and place in preservation solution for 2 h at 4 °C.

Recipient operation ● TIMING 60–70 min

13| Anesthetize the B10A (H-2^a) or CBA/J (H-2^k) mouse with i.p. ketamine (50 mg kg^{-1}) and xylazine (10 mg kg^{-1}).

14| Place the mouse under an operating microscope at a magnification of ×6–25.

15| Make a long midline abdominal incision from pubis to xyphoid.

16| Expose the abdominal cavity using a micro-retractor.

17| Retract the intestines superiorly and cover with wet gauze.

18| Move the reproductive organs (testes, epididymis and seminal vesicles) inferiorly and cover with wet gauze.
? TROUBLESHOOTING

19| Divide the avascular mesentery of the sigmoid colon using a large micro-tweezer at a 45° angle.

20| Pass a strip of wet gauze under the sigmoid colon, and use it to retract the sigmoid colon to the left side of the abdomen.

21| Expose the abdominal aorta and the IVC between the renal vessels and the iliac bifurcation using cotton swabs and micro-bipolar forceps.

22| Ligate one or two groups of the lumbar vessels originating from the exposed great vessels using 5-0 silk sutures. This procedure has not caused either limb paresis or reduced recipient survival in our hands, though if these were observed after the operation, aortic occlusion would need to be considered. Although not tested directly, ligation of these vessels using thinner (6-0 or 7-0) silk suture is also likely to be a reasonable alternative to the use of 5-0 silk.
? TROUBLESHOOTING

23| Place micro-clips on the distal and proximal sides of the exposed great vessels to interrupt the blood flow.
? TROUBLESHOOTING

24| Make an aortotomy (surgical incision into the aorta) in the abdominal aorta using a 30-gauge needle, and extend this longitudinally using micro-spring scissors.
▲ CRITICAL STEP The aortotomy should be the same size as the orifice of the donor ascending aorta or slightly smaller.

25| Place the donor heart into the right side of the abdomen in an orientation that allows the pulmonary artery to run underneath the aorta and perpendicular to the clamped vessels. Cover the donor heart with a gauze moistened with cold solution and drip the cold solution on the gauze several times during anastomosis (surgical connection of two blood vessels).

26| Using a small micro-tweezer at a 45° angle as a needle holder, anastomose the donor aorta to the recipient abdominal aorta in an end-to-side fashion using 10-0 nylon on a 4-mm (3/8) needle. Placement of anchor stitches on the proximal and distal side of the aortotomy facilitates this step.

27| Complete the left side of the anastomosis first using a continuous running suture that utilizes the nylon of the distal anchor stitch. Finish with a tie to the nylon of the proximal anchor stitch.
▲ CRITICAL STEP The continuous suture should run for four to five stitches in a counter-clockwise direction from distal to proximal side.

28| Flip over the heart by flipping it into the left side of the abdomen.

29| Complete the right side of the anastomosis using a continuous running suture that makes use of the nylon suture from the proximal anchor stitch. Finish with a tie to the nylon of the distal anchor stitch.
▲ CRITICAL STEP The continuous suture should run for four to five stitches in a counter-clockwise direction from proximal to distal side. The stitches should be evenly distributed and the edge distances should be kept constant.
? TROUBLESHOOTING

30| Fill the IVC partially with blood by temporarily releasing the distal clamp.

31| Make a small hole venotomy (surgical incision into the vein) in the IVC using a micro-spring scissors, and extend transversely using a small micro-tweezer at a 45° angle.
▲ CRITICAL STEP The venotomy should be separated from the aortotomy, at the level just inferior to the aortotomy. The extended hole should be the same size as the orifice of the donor pulmonary artery or slightly larger.

32| Complete the right side of the anastomosis first using a continuous running suture that utilizes the nylon of the distal anchor stitch. Finish with a tie to the nylon of the proximal anchor stitch.
▲ CRITICAL STEP In contrast to the aortic anastomoses, the continuous suture should run for five to six stitches in a clockwise direction from distal side to proximal side.

33| Flip over the heart by flipping it into the right side of the abdomen.

34| Complete the left side of the anastomosis using a continuous running suture that makes use of the nylon suture from the proximal anchor stitch. Finish with a tie to the nylon of the distal anchor stitch.
▲ CRITICAL STEP The continuous suture should run for five to six stitches in a clockwise direction from proximal side to distal side.

35| Release the distal clamp first to allow retrograde blood flow into the graft.

36| Inspect the anastomotic sites for bleeding by a temporary release of the proximal clamp.
? TROUBLESHOOTING

37| After ascertaining satisfactory hemostasis, release the proximal clamp.
▲ CRITICAL STEP The warm ischemic time of the donor heart (Steps 25–37) is approximately 30 min. After declamping, a short episode of fibrillation following reperfusion in the transplanted heart is seen, which then usually converts into sinus rhythm spontaneously.
? TROUBLESHOOTING

38| Return the intestines and reproductive organs to the abdominal cavity.

39| Close the abdominal incision using a continuous running suture using 5-0 nylon on a 16-mm (3/8) needle.

40| Place the recipient mouse into a warming cage to recover.
? TROUBLESHOOTING

41| Remove the nylon suture used to close the abdominal incision 14 d after surgery. Alternatively, resorbable suture material may be used.

Method for scoring grafts ● TIMING 1 min (per day)

42| During the 60-d observation period, perform manual palpation every day to gauge graft rejection or survival. The cardiac grafts should be judged by a blinded investigator and a score should be given based on the presence or absence of regular contractions. The scoring system we use was developed in a previous study[40,41] and utilizes values from 0 to 3, where 3 indicates a strong contraction and a soft graft with little turgor, 2 indicates a mild contraction and mildly hard turgor, 1 indicates a weak contraction and hard turgor and 0 indicates no contraction.

Method for murine echocardiography ● TIMING 30 min

43| During the 60-d observation period, perform murine echocardiography at each study point to evaluate graft contraction. Anesthetize the recipient mouse with i.p. ketamine (50 mg kg^{-1}) and xylazine (10 mg kg^{-1}). Alternatively, inhaled isoflurane may be used.
? TROUBLESHOOTING

44| Shave the dorsolumbar region of the back.

45| Hold the mouse in prone position in your off-hand.

46| Obtain echocardiographic images at a depth of 3 cm with a 120-Hz frame rate.

47| Image the heart in the 2D long-axis view.

48| Place the M-mode cursor vertically to the interventricular septum and posterior wall of the LV at the level of the papillary muscles. Measure the heart rate, LV internal diameter at end-diastole (LVDD) and end-systole (LVDS), as well as the interventricular septal and posterior wall thicknesses. Repeat the measurements at least five times, and calculate the average.

49| Calculate the percentage fractional shortening (%FS) using the following formula:

$$\%\mathrm{FS} = \frac{(\mathrm{LVDD} - \mathrm{LVDS})}{\mathrm{LVDD}} \times 100.$$

50| Image the heart in the 2D short-axis view. The LV internal end-diastolic area (EDA) and end-systolic area (ESA) are measured at the mid-papillary muscle level by tracing the endocardial contour. Repeat the measurements at least five times, and calculate the average. Sample 2D echocardiographic images and endocardial trace contours are shown in **Figure 2**.

51| Calculate the percentage fractional area change (%FAC) using the following formula:

$$\%\mathrm{FAC} = \frac{(\mathrm{EDA} - \mathrm{ESA})}{\mathrm{EDA}} \times 100.$$

Method for perfusion-fixation of the heart ● TIMING 15 min

52| At 60 d after transplantation, anesthetize the recipient mouse with i.p. ketamine (50 mg kg^{-1}) and xylazine (10 mg kg^{-1}).

53| Perform a midline thoracotomy and laparotomy.

54| Expose the native heart and transplanted heart.

55| Insert a 21-gauge Surflo winged cannula into the LV of the recipient native heart and open the right atrium of the recipient native heart to allow blood to be washed out by the perfusion solution.

56| Perfuse the mouse with 10 ml 1× PBS at 2 ml min^{-1} using a KDS-100 infusion pump.

57| Perfuse the mouse with 10 ml 10% formaldehyde at a rate of 2 ml min^{-1} using the pump. The fixation is complete when the mouse becomes rigid.

58| Harvest the transplanted heart.

Method for staining and histomorphometric assessment of vessels ● TIMING 120 min

59| Fix the harvested heart in 10% formalin.

60| Embed the harvested heart in paraffin.

61| Section the harvested heart transversely at the maximal circumference of the ventricle, and cut 5-μm sections.

62| Stain some sections with H&E.

63| Stain some sections with elastica van Gieson to highlight the IEL.

64| Use the H&E-stained sections to assess rejection using a modified form of the criteria of the Working Formulation of the International Society for Heart and Lung Transplantation[42,43]. Grading is from 0 to 3, depending on the amount of mononuclear cell infiltration. A grade of 0 indicates no infiltration, 1 indicates faint and limited infiltration, 2 indicates moderate infiltration and 3 indicates severe infiltration.

65| Photograph elastin-stained cross-sections of the coronary arteries with a well-defined smooth muscle cell layer and IEL in the vascular wall using a Sony DXC-960 MD 3CCD color camera affixed on top of an Olympus imaging microscope.

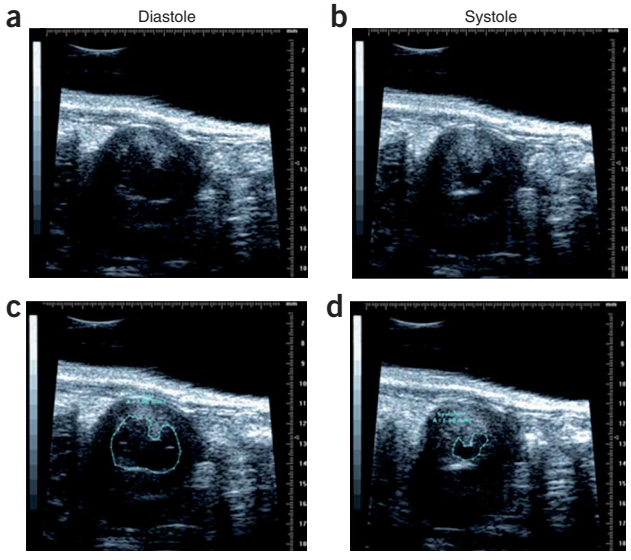

Figure 2 | Echocardiographic assessment of cardiac graft function, performed on a transplanted mouse heart using a 30-mHz transducer. Freeze-frame images at end-diastole (**a**) and end-systole (**b**) permit calculation of percentage fractional area change (%FAC) as a measure of contractile function, and left ventricular mass. Sample endocardial contour tracings are shown in the lower set of images at end-diastole (**c**) and end-systole (**d**). Note the papillary muscle at the superior aspect of the tracing.

66| Process digital images using Image-Pro Plus software and trace the area encompassed by the lumen and IEL. Sample trace contours, which enable calculation of CAV, are shown in **Figure 3**.

67| Calculate each planimetered area using image analysis software.

68| The area of luminal stenosis in each section should be calculated according to the following formula:

$$\text{Luminal occlusion } (\%) = \frac{\text{IEL area} - \text{luminal area}}{\text{IEL area}} \times 100.$$

Examples of vessels that have developed minimal, intermediate and severe degrees of CAV are shown in **Figure 4**.

? TROUBLESHOOTING

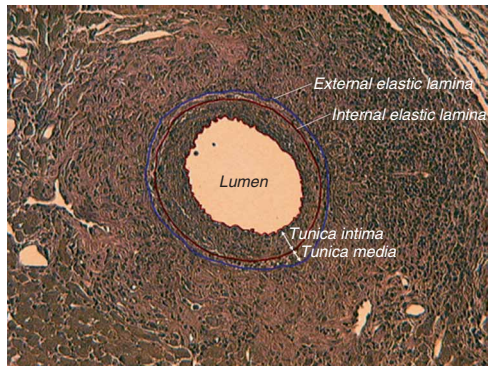

Figure 3 | Sample histomorphometric tracing for determination of CAV. Elastin-stained vessel is shown, with sample trace contours indicated. Image analysis software, such as NIH Image, can be used to determine planimetered areas encompassed by the various trace contours.

69| An independent observer should calculate the severity of CAV and parenchymal rejection. This person should be blinded to the treatment protocol. Report scores as either the mean rejection score or the mean ± s.e.m. percentage luminal occlusion score.

? TROUBLESHOOTING

Troubleshooting advice can be found in **Table 1**.

TABLE 1 | Troubleshooting table.

Step	Problem	Possible reason	Solution
18	The urinary bladder obstructs the operative view	The urinary bladder is full of urine	Bladder should be emptied with gentle pressure
22	Bleeding has occurred from the lumbar or small vessels	Injury of the lumbar or small vessels	This is usually managed by compression with gauze or cotton swabs
23	The inferior vena cava continues to be filled with blood after clamping	Missed or loose ligation of the lumbar vessels	The ligation of lumbar vessels should be rechecked
29	Limb paresis is observed bilaterally after operation	Aortic occlusion at the anastomotic site	This is an undesirable and rare occurrence, but if observed it requires humane killing of the experimental animal
36	Bleeding at the anastomotic sites following a release of the proximal clamp	Inadequate anastomosis	Oozing is managed by compression with small pieces of an absorbable gelatin sponge. Active bleeding is stopped by placing additional sutures
37	The donor heart appears plethoric, red and turgid (congested)	Poor drainage of the venous effluent from the perfusion donor coronary arteries at the IVC anastomosis, which is the typical site of flow restriction	The position of the donor heart should be checked to avoid torsion
40	The blood loss is severe during the operation	Inadequate anastomosis, nicked vessels, or hemostatic diathesis	1 ml saline solution can be injected s.c.
43	Bradycardia and a low cardiac output state	Several anesthetic agents such as pentobarbital, tribromoetanol, isoflurane, and a combination of ketamine and xylazine are used by investigators to anesthetize mice before echocardiographic evaluation of cardiac function. These anesthetic agents have the potential to affect cardiac performance and hemodynamics	Isoflurane and pentobarbital may minimize such side effects, and may be the agents of choice for anesthesia before evaluation of cardiac performance[72,73]
68	False elevation of luminal occlusion	Extrinsic compression of vessels, typically venules, during tissue preparation	To avoid this artifact, restrict analysis primarily to round vessels observed in cross-section

ANTICIPATED RESULTS

The success rate (defined as immediate postoperative functioning of the graft) for heterotopic murine cardiac transplantation in our hands has been 96.2%. All successful allografts have survived to the pre-specified 60-d endpoint, likely because all recipients were immunosuppressed by pre-operative administration of antimurine CD4 (clone GK 1.5) and anti-CD8 (clone 2.43) Abs.

Scientific uses of the model

The heterotopic cardiac transplantation model has proved a reliable means of investigating diagnostic and therapeutic interventions for both acute and chronic allograft vasculopathy. Histologically, the acute allograft vasculopathy of coronary arteries is characterized by inflammatory cell migration and adhesion, without many smooth muscle cells present within the intima. This early arterial injury is followed later by a luminal narrowing marked by infiltration of lymphocytes and macrophages, coupled with smooth muscle cells. Thus, the migration of the smooth muscle cells into the lumen contributes to the development of CAV, which eventuates in a diffuse concentric luminal narrowing of the entire coronary arterial tree (**Fig. 4c–f**). Over time, the infiltration of lymphocytes and macrophages decreases. The development of CAV is induced by an immune-mediated process modified by non-immunological factors. When isograft experiments were performed with immediate transplantation, without an intervening cold preservation period, little if any luminal narrowing was observed (**Fig. 4a, b**)[41]. Many important insights have been gained over past years into the mechanisms underlying CAV. The importance of T-lymphocyte activation and cellular rejection has been demonstrated in heterotopic cardiac heart transplantation. Depletion of $CD4^+$ (ref. 44) and $CD8^+$ (ref. 45) T lymphocytes prevented the development of CAV. Co-stimulatory signaling pathways such as CD28-B7 (refs. 46,47), CD40-CD154 (ref. 48) and CD27-CD70 (ref. 49), which play crucial roles in T-lymphocyte activation, have been implicated in the pathogenesis of CAV, through the use of a heterotopic cardiac allotransplant model. After activation, T lymphocytes produce a variety of cytokines such as interleukin-2 (ref. 50), interferon-10 (ref. 51), interferon-γ (ref. 52) and tumor necrosis factor-α[53], which were also shown to be involved in the development of CAV. Expression of intercellular adhesion molecule-1 (ICAM-1)[54] and vascular cell adhesion molecule-1 (VCAM-1)[55] was shown to be enhanced in the area of CAV. Cardiac graft ICAM-1 mediated primary graft failure[56], and treatment with mAbs of ICAM-1 and leukocyte function–associated antigen-1 caused a significant suppression of CAV[57].

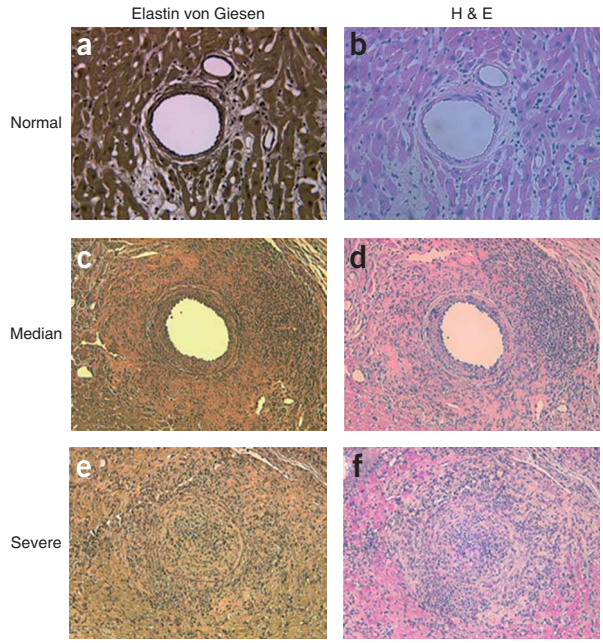

Figure 4 | Representative histology of cardiac allograft vasculopathy (CAV). Two staining methods are shown. Elastin staining (left set of panels) and H&E staining (right set of panels). Examples of varying degrees of CAV severity are shown: (**a**,**b**) normal, (**c**,**d**) median, (**e**,**f**) severe. Elastin staining allows definition of intimal/medial boundaries, whereas H&E staining better defines leukocyte infiltration and myocytolysis.

In the presence of cytokines and adhesion molecules, a variety of growth factors are secreted from activated endothelial cells and infiltrating cells. Transforming growth factor-β-1 has also correlated with the development of CAV[58], and platelet-derived growth factor[59] and connective tissue growth factor[60] accelerate the formation of CAV. Chemokines and chemokine receptors are critical in leukocyte recruitment, activation and differentiation. Among them, CC chemokine receptors 1 and 5 and CXC chemokine receptor 3 have been reported to play important roles in the development of CAV[61,62]. Moreover, the roles of cyclic adenosine monophosphate[41], early growth response gene-1 (ref. 63), cyclin-dependent kinase 2 kinase[64], signal transducer and activator of transcription[65], heme oxygenase-1 (ref. 66), nitric oxide[67] and apolipoprotein-E[68] were elucidated in allograft vasculopathy using the heterotopic heart transplant model. Recently, this model has been used to develop a means of identifying acute rejection through bioluminescence imaging of trafficking passenger leukocytes[69] and to study the benefit of decreasing asymmetric dimethylarginine levels[70] and increasing superoxide dismutase 1 levels[71] in chronic graft coronary artery disease. These are just a few of the myriad cases where the heterotopic cardiac transplant model has proven useful. If antimurine CD4 and anti-CD8 Abs are not administered to recipient mice pre-operatively, it is also possible to study immune tolerance or just allograft rejection using this protocol.

Conclusion

Cardiac transplantation has become the treatment of choice for patients with end-stage heart failure. Acute and chronic CAV is a common and serious post-transplantation disease that often presents silently. Murine heterotopic cardiac

transplantation reliably reproduces the histological, immunological and non-immunological manifestations of CAV. Using this model, investigators are currently exploring means of diagnosing and treating the vasculopathy that places transplanted hearts at risk.

ACKNOWLEDGMENTS This work was supported in part by National Institutes of Health grants HL55397 and HL085149, as well as the Scleroderma Research Foundation.

COMPETING INTERESTS STATEMENT The authors declare that they have no competing financial interests.

Published online at http://www.natureprotocols.com
Reprints and permissions information is available online at http://npg.nature.com/reprintsandpermissions

1. Steinman, T.I. *et al.* Guidelines for the referral and management of patients eligible for solid organ transplantation. *Transplantation* **71**, 1189–1204 (2001).
2. Orens, J.B. *et al.* Thoracic organ transplantation in the United States, 1995–2004. *Am. J. Transplant.* **6**, 1188–1197 (2006).
3. Taylor, D.O. *et al.* Registry of the International Society for Heart and Lung Transplantation: twenty-third official adult heart transplantation report—2006. *J. Heart Lung Transplant.* **25**, 869–879 (2006).
4. Gao, S.Z. *et al.* Acute myocardial infarction in cardiac transplant recipients. *Am. J. Cardiol.* **64**, 1093–1097 (1989).
5. Stoica, S.C., Goddard, M. & Large, S.R. The endothelium in clinical cardiac transplantation. *Ann. Thorac. Surg.* **73**, 1002–1008 (2002).
6. Uehara, S. *et al.* NK cells can trigger allograft vasculopathy: the role of hybrid resistance in solid organ allografts. *J. Immunol.* **175**, 3424–3430 (2005).
7. Billingham, M.E. Histopathology of graft coronary disease. *J. Heart Lung Transplant.* **11**, S38–S44 (1992).
8. Weis, M. & von Scheidt, W. Coronary artery disease in the transplanted heart. *Annu. Rev. Med.* **51**, 81–100 (2000).
9. Barnard, C.N. The operation. A human cardiac transplant: an interim report of a successful operation performed at Groote Schuur Hospital, Cape Town. *S. Afr. Med. J.* **41**, 1271–1274 (1967).
10. Kadner, A., Chen, R.H. & Adams, D.H. Heterotopic heart transplantation: experimental development and clinical experience. *Eur. J. Cardiothorac. Surg.* **17**, 474–481 (2000).
11. Carrel, A. & Guthrie, C.C. The transplantation of veins and organs. *Am. Med.* **10**, 1101–1102 (1905).
12. Mann, F.C., Priestley, J.T., Markowitz, J. & Yater, W.M. Transplantation of the intact mammalian heart. *Arch. Surg.* **26**, 219–224 (1933).
13. Chiba, C. *et al.* Studies on the transplanted heart. Its metabolism and histology. *J. Exp. Med.* **115**, 853–866 (1962).
14. Heron, I. A technique for accessory cervical heart transplantation in rabbits and rats. *Acta Pathol. Microbiol. Scand. [A]* **79**, 366–372 (1971).
15. Marcus, E., Wong, S.N. & Luisada, A.A. Homologous heart grafts. I. Technique of interim parabiotic perfusion. II. Transplantation of the heart in dogs. *AMA Arch. Surg.* **66**, 179–191 (1953).
16. Neptune, W.B., Cookson, B.A., Bailey, C.P., Appler, R. & Rajkowski, F. Complete homologous heart transplantation. *AMA Arch. Surg.* **66**, 174–178 (1953).
17. Sayegh, S.F., Creech, O. Jr. & Harding, J.H. Transplantation of the homologous heart. *Surg. Forum* **8**, 317–319 (1957).
18. Fulmer, R.I., Cramer, A.T., Liebelt, R.A. & Liebelt, A.G. Transplantation of cardiac tissue into the mouse ear. *Am. J. Anat.* **113**, 273–285 (1963).
19. Judd, K.P. & Trentin, J.J. Cardiac transplantation in mice. I. Factors influencing the take and survival of heterotopic grafts. *Transplantation* **11**, 298–302 (1971).
20. Giardina, J.J. *et al.* Use of cyclosporine in the mouse heterotopic heart transplant model. *J. Heart Transplant.* **9**, 106–113 (1990).
21. Koehl, G.E. *et al.* Rapamycin protects allografts from rejection while simultaneously attacking tumors in immunosuppressed mice. *Transplantation* **77**, 1319–1326 (2004).
22. Mazer, S.P. & Pinsky, D.J. Alive and kicking: endothelium at the geographic nexus of vascular rejection. *Circ. Res.* **91**, 1085–1088 (2002).
23. Abbott, C.P., Lindsey, E.S., Creech, O. Jr. & Dewitt, C.W. A technique for heart transplantation in the rat. *Arch. Surg.* **89**, 645–652 (1964).
24. Ono, K. & Lindsey, E.S. Improved technique of heart transplantation in rats. *J. Thorac. Cardiovasc. Surg.* **57**, 225–229 (1969).
25. Corry, R.J., Winn, H.J. & Russell, P.S. Primarily vascularized allografts of hearts in mice. The role of H-2D, H-2K, and non-H-2 antigens in rejection. *Transplantation* **16**, 343–350 (1973).
26. Asfour, B. *et al.* A simple new model of physiologically working heterotopic rat heart transplantation provides hemodynamic performance equivalent to that of an orthotopic heart. *J. Heart Lung Transplant.* **18**, 927–936 (1999).
27. Chen, Z.H. A technique of cervical heterotopic heart transplantation in mice. *Transplantation* **52**, 1099–1101 (1991).
28. Matsuura, A., Abe, T. & Yasuura, K. Simplified mouse cervical heart transplantation using a cuff technique. *Transplantation* **51**, 896–898 (1991).
29. Tomita, Y. *et al.* Improved technique of heterotopic cervical heart transplantation in mice. *Transplantation* **64**, 1598–1601 (1997).
30. Niimi, M. The technique for heterotopic cardiac transplantation in mice: experience of 3000 operations by one surgeon. *J. Heart Lung Transplant.* **20**, 1123–1128 (2001).
31. Iwanaga, K. *et al.* Riboflavin-mediated reduction of oxidant injury, rejection, and vasculopathy following cardiac allotransplantation. *Transplantation* (in press).
32. Medawar, P.B. The behavior and fate of skin autografts and skin homografts in rabbits. *J. Anat.* **78**, 176–179 (1944).
33. Felix, N.J. *et al.* H2-DMalpha$^{(-/-)}$ mice show the importance of major histocompatibility complex-bound peptide in cardiac allograft rejection. *J. Exp. Med.* **192**, 31–40 (2000).
34. George, J.F., Pinderski, L.J., Litovsky, S. & Kirklin, J.K. Of mice and men: mouse models and the molecular mechanisms of post-transplant coronary artery disease. *J. Heart Lung Transplant.* **24**, 2003–2014 (2005).
35. Eichwald, E.J., Silmser, C.R. & Weissman, I. Sex-linked rejection of normal and neoplastic tissue. I. Distribution and specificity. *J. Natl. Cancer Inst.* **20**, 563–575 (1958).
36. Bailey, D.W. Allelic forms of a gene controlling the female immune response to the male antigen in mice. *Transplantation* **11**, 426–428 (1971).
37. Bailey, D.W. & Hoste, J. A gene governing the female immune response to the male antigen in mice. *Transplantation* **11**, 404–407 (1971).
38. Furukawa, Y., Mandelbrot, D.A., Libby, P., Sharpe, A.H. & Mitchell, R.N. Association of B7-1 co-stimulation with the development of graft arterial disease. Studies using mice lacking B7-1, B7-2, or B7-1/B7-2. *Am. J. Pathol.* **157**, 473–484 (2000).
39. Russell, P.S., Chase, C.M., Winn, H.J. & Colvin, R.B. Coronary atherosclerosis in transplanted mouse hearts. I. Time course and immunogenetic and immunopathological considerations. *Am. J. Pathol.* **144**, 260–274 (1994).
40. Pinsky, D. *et al.* Restoration of the cAMP second messenger pathway enhances cardiac preservation for transplantation in a heterotopic rat model. *J. Clin. Invest.* **92**, 2994–3002 (1993).
41. Wang, C.Y. *et al.* cAMP pulse during preservation inhibits the late development of cardiac isograft and allograft vasculopathy. *Circ.Res.* **86**, 982–988 (2000).
42. Billingham, M.E. *et al.* A working formulation for the standardization of nomenclature in the diagnosis of heart and lung rejection: Heart Rejection Study Group. The International Society for Heart Transplantation. *J. Heart Transplant.* **9**, 587–593 (1990).
43. Stewart, S. *et al.* Revision of the 1990 working formulation for the standardization of nomenclature in the diagnosis of heart rejection. *J. Heart Lung Transplant.* **24**, 1710–1720 (2005).
44. Szeto, W.Y. *et al.* Depletion of recipient CD4$^+$ but not CD8$^+$ T lymphocytes prevents the development of cardiac allograft vasculopathy. *Transplantation* **73**, 1116–1122 (2002).
45. Schnickel, G.T. *et al.* CD8 lymphocytes are sufficient for the development of chronic rejection. *Transplantation* **78**, 1634–1639 (2004).
46. Glysing-Jensen, T., Raisanen-Sokolowski, A., Sayegh, M.H. & Russell, M.E. Chronic blockade of CD28-B7-mediated T-cell costimulation by CTLA4Ig reduces intimal thickening in MHC class I and II incompatible mouse heart allografts. *Transplantation* **64**, 1641–1645 (1997).
47. Larsen, C.P. *et al.* Long-term acceptance of skin and cardiac allografts after blocking CD40 and CD28 pathways. *Nature* **381**, 434–438 (1996).
48. Wang, C.Y. *et al.* Suppression of murine cardiac allograft arteriopathy by long-term blockade of CD40–CD154 interactions. *Circulation* **105**, 1609–1614 (2002).
49. Yamada, A. *et al.* CD70 signaling is critical for CD28-independent CD8$^+$ T cell-mediated alloimmune responses *in vivo*. *J. Immunol.* **174**, 1357–1364 (2005).

50. Zand, M.S. *et al.* Interleukin-2 and interferon-gamma double knockout mice reject heterotopic cardiac allografts. *Transplantation* **70**, 1378–1381 (2000).
51. Fischbein, M.P. *et al.* Regulated interleukin-10 expression prevents chronic rejection of transplanted hearts. *J. Thorac. Cardiovasc. Surg.* **126**, 216–223 (2003).
52. Nagano, H. *et al.* Interferon-gamma deficiency prevents coronary arteriosclerosis but not myocardial rejection in transplanted mouse hearts. *J. Clin. Invest.* **100**, 550–557 (1997).
53. McKee, C.M. *et al.* Prolonged allograft survival in TNF receptor 1-deficient recipients is due to immunoregulatory effects, not to inhibition of direct antigraft cytotoxicity. *J. Immunol.* **168**, 483–489 (2002).
54. Dietrich, H. *et al.* Mouse model of transplant arteriosclerosis: role of intercellular adhesion molecule-1. *Arterioscler. Thromb. Vasc. Biol.* **20**, 343–352 (2000).
55. Ardehali, A., Laks, H., Drinkwater, D.C., Ziv, E. & Drake, T.A. Vascular cell adhesion molecule-1 is induced on vascular endothelia and medial smooth muscle cells in experimental cardiac allograft vasculopathy. *Circulation* **92**, 450–456 (1995).
56. Wang, C.Y. *et al.* Cardiac graft intercellular adhesion molecule-1 (ICAM-1) and interleukin-1 expression mediate primary isograft failure and induction of ICAM-1 in organs remote from the site of transplantation. *Circ. Res.* **82**, 762–772 (1998).
57. Russell, P.S., Chase, C.M. & Colvin, R.B. Coronary atherosclerosis in transplanted mouse hearts. IV effects of treatment with monoclonal antibodies to intercellular adhesion molecule-1 and leukocyte function-associated antigen-1. *Transplantation* **60**, 724–729 (1995).
58. Densem, C.G., Hutchinson, I.V., Cooper, A., Yonan, N. & Brooks, N.H. Polymorphism of the transforming growth factor-beta 1 gene correlates with the development of coronary vasculopathy following cardiac transplantation. *J. Heart Lung. Transplant.* **19**, 551–556 (2000).
59. Mancini, M.C. & Evans, J.T. Role of platelet-derived growth factor in allograft vasculopathy. *Ann. Surg.* **231**, 682–688 (2000).
60. Csencsits, K. *et al.* Transforming growth factor beta-induced connective tissue growth factor and chronic allograft rejection. *Am. J. Transplant.* **6**, 959–966 (2006).
61. Akashi, S. *et al.* A novel small-molecule compound targeting CCR5 and CXCR3 prevents acute and chronic allograft rejection. *Transplantation* **80**, 378–384 (2005).
62. Yun, J.J. *et al.* Combined blockade of the chemokine receptors CCR1 and CCR5 attenuates chronic rejection. *Circulation* **109**, 932–937 (2004).
63. Okada, M. *et al.* Transcriptional control of cardiac allograft vasculopathy by early growth response gene-1 (*Egr*-1). *Circ. Res.* **91**, 135–142 (2002).
64. Suzuki, J. *et al.* Prevention of graft coronary arteriosclerosis by antisense cdk2 kinase oligonucleotide. *Nat. Med.* **3**, 900–903 (1997).
65. Koglin, J., Glysing-Jensen, T., Gadiraju, S. & Russell, M.E. Attenuated cardiac allograft vasculopathy in mice with targeted deletion of the transcription factor STAT4. *Circulation* **101**, 1034–1039 (2000).
66. Yamashita, K. *et al.* Heme oxygenase-1 is essential for and promotes tolerance to transplanted organs. *FASEB J.* **20**, 776–778 (2006).
67. Weis, M. & Cooke, J.P. Cardiac allograft vasculopathy and dysregulation of the NO synthase pathway. *Arterioscler. Thromb. Vasc. Biol.* **23**, 567–575 (2003).
68. Russell, P.S., Chase, C.M. & Colvin, R.B. Accelerated atheromatous lesions in mouse hearts transplanted to apolipoprotein-E-deficient recipients. *Am. J. Pathol.* **149**, 91–99 (1996).
69. Tanaka, M. *et al.* *In vivo* visualization of cardiac allograft rejection and trafficking passenger leukocytes using bioluminescence imaging. *Circulation* **112**, I105–I110 (2005).
70. Tanaka, M. *et al.* Dimethylarginine dimethylaminohydrolase overexpression suppresses graft coronary artery disease. *Circulation* **112**, 1549–1556 (2005).
71. Tanaka, M. *et al.* Overexpression of human copper/zinc superoxide dismutase (SOD1) suppresses ischemia-reperfusion injury and subsequent development of graft coronary artery disease in murine cardiac grafts. *Circulation* **110**, II200–II206 (2004).
72. Janssen, B.J. *et al.* Effects of anesthetics on systemic hemodynamics in mice. *Am. J. Physiol. Heart Circ. Physiol.* **287**, H1618–H1624 (2004).
73. Kawahara, Y. *et al.* Preferable anesthetic conditions for echocardiographic determination of murine cardiac function. *J. Pharmacol. Sci.* **99**, 95–104 (2005).